

Negative coercivity in epitaxially grown (110) DyFe₂/YFe₂ superlattices

J.-M. L. Beaujour, S. N. Gordeev, G. J. Bowden, P. A. J. de Groot,^{a)} and B. D. Rainford
Department of Physics and Astronomy, University of Southampton, SO17 1BJ, United Kingdom

R. C. C. Ward and M. R. Wells
Clarendon Laboratory, Oxford University, Oxford OX1 3PU, United Kingdom

(Received 2 August 2000; accepted for publication 29 November 2000)

Molecular beam epitaxial methods have been used to grow single crystal Laves phase DyFe₂/YFe₂ superlattice samples with a (110) growth direction. Detailed magnetization curves have been obtained for YFe₂ dominated multilayer samples [*w*DyFe₂/*4w*YFe₂] \times 16 with *w* = 45, 50, and 55 Å. In particular, it is shown that the formation of magnetic exchange springs in the magnetically soft YFe₂ layers, can be used to engineer multilayer samples with a negative coercivity. Further, by using asymmetric field cycling procedures, we have investigated the irreversible parts of the *M*–*B* loop, associated with the switching of the DyFe₂ multilayers. © 2001 American Institute of Physics. [DOI: 10.1063/1.1344594]

Recently, it has been shown that the magnetic properties of epitaxially grown (110) multilayers of DyFe₂/YFe₂ can be engineered with specific magnetic properties. In particular, films have been produced with (i) magnetic compensation points,¹ (ii) tailored coercive fields² within the limits $B_C(\text{DyFe}_2) \leq B_C \leq \infty$, and (iii) model magnetic exchange springs, that scale closely with $1/d^2$, where *d* is the width of the magnetically soft YFe₂ layers.³ In this letter we will show that by utilizing the properties of magnetic exchange springs, it is possible to grow YFe₂ dominated films with a tailored negative coercivity. Such films should find applications in devices that require specified exchange bias fields, such as magnetostrictive and spintronic devices.^{4,5}

The problem of inverted magnetic hysteresis loops, in sputtered multilayer films, has been of increasing interest in recent years.^{6–12} In the main, such behavior has been attributed to “exchange-field biasing” across the interface between two layers, characterized by different magnetic hardness and coupled antiferromagnetically. Examples are: (i) CoO–Co composite films,^{6,7} (ii) δ -MnGa/(Mn, Ga, As)/ δ -MnGa trilayer films,⁸ (iii) Gd–Fe/Tb–Fe bilayer films,⁹ (iv) Gd/Co bilayer films,¹⁰ and (v) NiFe/TbCo bilayer films.¹¹ Finally, it should be noted that a different mechanism, other than exchange-field biasing, has been proposed in Ref. 12. In the latter, dipolar fields emanating from the hard magnetic layers demagnetize the soft layers, giving rise to negative coercivities.

In this letter, another mechanism for engineering multilayer samples with negative coercivity is demonstrated. Unlike previous work, this mechanism is based primarily on the properties of magnetic exchange springs, which “unwind,” and ultimately disappear, as the applied field approaches the critical bending field B_B .^{13–16} The effect is demonstrated using epitaxial, YFe₂ dominated, superlattices [*w*DyFe₂/*4w*YFe₂] \times 16 with *w* = 45, 50, and 55 Å, grown by molecular beam epitaxial (MBE) methods. It is shown that magnetic exchange springs in the YFe₂ layers are re-

sponsible for (i) the negative coercive field, and (ii) the reversible parts of the magnetic hysteresis loop. By way of contrast, the irreversible parts of the *M*–*B* loop are associated with the switching of the DyFe₂ layers.

Details of the cubic Laves O_h^7 -*F3dm* intermetallic compounds DyFe₂ and YFe₂ can be found in various review articles (e.g., Refs. 17 and 18). These compounds have high Curie temperatures ($T_C \approx 600$ K), due to the strong Fe–Fe exchange interactions. The Dy–Fe exchange interactions give rise to antiferromagnetic coupling between the Dy and Fe moments. The direction of easy magnetization is controlled by the crystal field interactions at the *RE* site.¹⁹ For bulk DyFe₂ the direction of magnetization is [001] at all temperatures, whereas for YFe₂ it is [111]. However, since YFe₂ is characterized by very weak magnetic anisotropy, it can be considered magnetically soft. Recent work has shown that the direction of magnetization in DyFe₂ thin films is temperature dependent,²⁰ probably due to lattice mismatch strains. Nevertheless, at temperatures below ~ 100 K, the direction of easy magnetization in MBE grown DyFe₂ films reverts to [001].^{1,20}

We used a Balzers UMS 630 ultrahigh vacuum facility to grow epitaxial DyFe₂/YFe₂ superlattice samples, by MBE techniques.^{1,20} The films were grown on epiprepared (11 $\bar{2}$ 0) sapphire substrates (10 \times 12 mm) with a 1000 Å (110) Nb buffer and a 30 Å layer of Fe. The films were grown by codeposition of elemental fluxes at a substrate temperature of 400 °C in (110) orientation, with the major axes parallel to those of niobium. Given that the bulk lattice parameters for DyFe₂ and YFe₂ are 7.325 and 7.363 Å, respectively, the mismatch at the superlattice interfaces is expected to be of the order 0.5%. *Ex situ* x-ray diffraction studies confirmed the single crystal nature of the samples. Superlattice satellites were clearly defined and confirmed the programmed repeat distances. In addition, high resolution transmission electron measurements indicate an interface roughness of less than 10 Å.²¹ Finally, we note that the superlattices are strained, both by their coherency strain, and thermal expansion mismatch with the substrate. For more details the reader is referred to Ref. 22.

^{a)}Electronic mail: pajdeg@phys.soton.uk

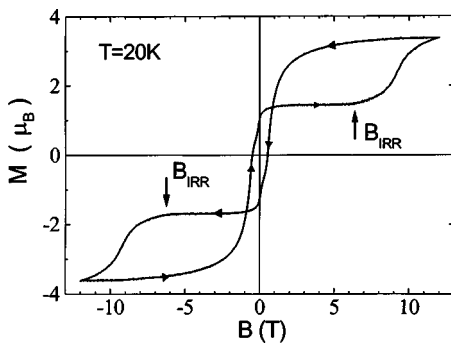


FIG. 1. In plane [001] magnetization curves for the superlattice film [50 Å DyFe₂/200 Å YFe₂] \times 16, obtained at $T=20$ K.

Magnetic hysteresis loops were measured using an Oxford Instruments Aerosonic 3001 vibrating sample magnetometer for $10\text{ K} < T < 300\text{ K}$ and for fields of up to 12 T applied along the [001] axis. A typical in plane magnetization curve, for $w = 50\text{ \AA}$, can be seen in Fig. 1. For convenience the magnetization M has been converted to Bohr magnetons per average formula unit ($\text{Dy}_{0.2}\text{Y}_{0.8}\text{Fe}_2$). Note that in going from -12 to $+12$ T, the magnetization crosses zero at $B_C = -0.50\text{ T}$. Thus, the film in question is characterized by a negative coercive field.

An interpretation of this data is summarized in Fig. 2. Here various schematic spin configurations can be seen, as a function of the applied magnetic field. In a large negative applied field (-12 T), the minimum energy state is achieved with the net moment of the DyFe₂ layers ($\sim 7\mu_B$ per formula unit) pointing along the applied field, as shown in Fig. 2(a). This means that magnetic exchange springs are necessarily set up in the thicker YFe₂ layers. However, as the strength of the applied field is reduced, the YFe₂ exchange springs unwind, until the applied field reaches a critical bending field B_B .¹³⁻¹⁶ For a symmetric exchange spring ($0^\circ \rightarrow \phi \rightarrow 0^\circ$) this bending field is determined by

$$B_B = B_{\text{EX}} \left(\frac{\pi}{N} \right)^2, \quad (1)$$

where (i) B_{EX} is the exchange field, and (ii) N is the number

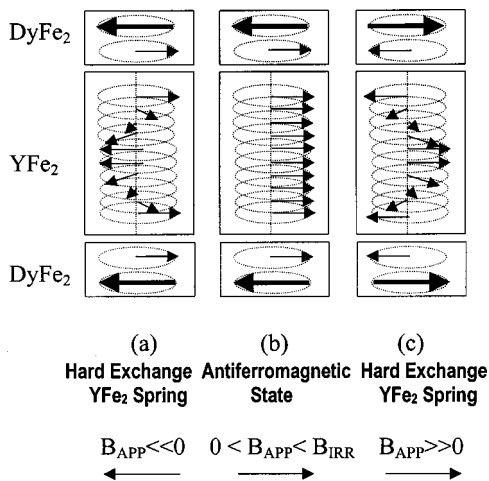


FIG. 2. Schematic representations of the magnetic moments and exchange springs in the [50 Å DyFe₂/200 Å YFe₂] \times 16 multilayer film, as the magnetic field is increased from a large negative to positive value. The large (small) arrows represent Dy (Fe) magnetic moments, respectively.

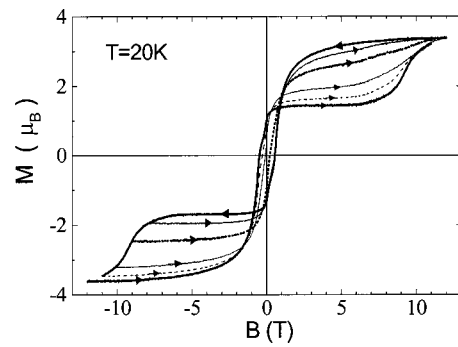


FIG. 3. In plane [001] magnetization curves for the sample [50 Å DyFe₂/200 Å YFe₂] \times 16 at $T=20$ K, for various asymmetric magnetic cycles (see text).

of monolayers in the spring.¹⁶ When the applied field falls below this value, the exchange spring becomes unstable to the creation of the antiferromagnetic state shown in Fig. 2(b). Since this state is characterized by a positive magnetic moment $\sim 1.0\mu_B$, the magnetization goes positive even though the applied field is still negative. Thus, the $M-B$ loop is characterized by a negative coercivity $B_C = -0.50\text{ T}$. Further support for this interpretation can be gleaned from the properties of exchange springs in DyFe₂/YFe₂ multilayer samples.³ Using the experimental data shown in Fig. 4 of Ref. 3, the predicted value of the bending field B_B is $\sim 0.75\text{ T}$, for a 200 Å thick YFe₂ layer. This is close to, but not identical to the measured coercivity of $B_C = -0.50\text{ T}$ for the sample in question. The difference may be due to penetration of the exchange springs in the DyFe₂ layers or interface roughness.

On increasing the field still further, the magnetic moment stays constant at $\sim 1.0\mu_B$ per formula unit, until the applied field exceeds a particular value B_{IRR} (the irreversibility field). Indeed, provided the magnetic field is not taken above B_{IRR} , the magnetization curve between -12 T and B_{IRR} is completely reversible. This is a clear signature of a magnetic exchange spring.¹³⁻¹⁶ However, when B_{IRR} is exceeded, the system becomes unstable to irreversible flips in the magnetic moments of the DyFe₂ layers, accompanied by the simultaneous creation of magnetic exchange springs in the YFe₂ layers. Finally, when all the DyFe₂ layers have been flipped over, we arrive at the spin configuration shown in Fig. 2(c).

By performing partial hysteresis loop measurements, we have been able to probe the irreversible nature of the flipping of the DyFe₂ layers. This can be done by first saturating the sample in a large positive magnetic field ($+12\text{ T}$) and subsequently reducing the field to B_{MIN} , before increasing the field back again to $+12\text{ T}$. The results of this asymmetric cycling procedure can be seen in Fig. 3. It can be seen that the degree of irreversibility is strongly dependent on the magnitude of B_{MIN} reached during this asymmetric magnetic cycle. For example, if the magnetic cycle is only taken to $B_{\text{MIN}} = -7\text{ T}$, the magnetization curve is practically reversible. This suggests therefore that all of the DyFe₂ layers remain pointing in the positive field direction, during the whole of this asymmetric magnetic cycle. However, when the field is taken below -7 T , increasing numbers of DyFe₂ layers are flipped over, presumably layer by layer. A possible

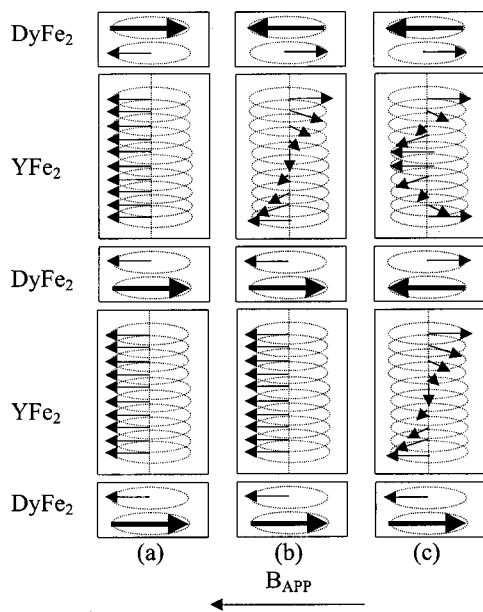


FIG. 4. Schematic representation of the successive reversals of DyFe_2 magnetic moments accompanied by the simultaneous creation of ($0 \rightarrow 180^\circ$) and ($0^\circ \rightarrow \phi \rightarrow 0^\circ$) magnetic exchange springs in the YFe_2 layers. Notations are the same as in Fig. 2.

interpretation of this effect is shown schematically in Fig. 4. For simplicity, only three DyFe_2 layers are shown in this diagram. Initially, we shall assume that the spin-configuration is in the antiferromagnetic state, illustrated in Fig. 4(a). Here all of the net moments of the DyFe_2 layers are pointing to the right. However, as the field is decreased to say below -7 T, the top DyFe_2 layer is flipped over. This event is accompanied by the simultaneous creation of a ($0 \rightarrow 180^\circ$) magnetic exchange spring in the neighboring YFe_2 layer, as shown in Fig. 4(b). As the field is further decreased, the next DyFe_2 layer is flipped over, resulting in the creation of a new ($0 \rightarrow 180^\circ$) exchange spring in the second YFe_2 layer, while the original ($0 \rightarrow 180^\circ$) exchange spring is converted into a ($0^\circ \rightarrow \phi \rightarrow 0^\circ$) exchange spring, as

illustrated in Fig. 4(c). Further experiments, with fewer multilayers, are in progress to see if this interpretation is correct.

This work has been supported by the Advanced Magnetism Program of the EPSRC and funded, in part, under Technology Group 4 (Materials and Structures) of the MoD Corporate Research Program.

- ¹M. Sawicki, G. J. Bowden, P. A. J. de Groot, B. D. Rainford, R. C. C. Ward, and M. R. Wells, *J. Appl. Phys.* **87**, 6839 (2000).
- ²M. Sawicki, G. J. Bowden, P. A. J. de Groot, B. D. Rainford, J.-M. L. Beaujour, R. C. C. Ward, and M. R. Wells, *Appl. Phys. Lett.* **77**, 573 (2000).
- ³M. Sawicki, G. J. Bowden, P. A. J. de Groot, B. D. Rainford, R. C. C. Ward, and M. R. Wells, *Phys. Rev. B* **62**, 5817 (2000).
- ⁴A. E. Clark, M. Wun-Fogle, J. P. Teter, J. B. Restorff, and S. F. Cheng, *J. Appl. Phys.* **76**, 7009 (1994).
- ⁵J. C. Lodder, D. J. Monsma, R. Vlutters, and T. Shimatsu, *J. Magn. Magn. Mater.* **198–199**, 119 (1999).
- ⁶C. Gao and M. J. O'Shea, *J. Magn. Magn. Mater.* **127**, 181 (1993).
- ⁷M. J. O'Shea and A. L. Al-Shariff, *J. Appl. Phys.* **75**, 6673 (1994).
- ⁸W. Van Roy, H. Akinaga, S. Miyayoshi, K. Tanaka, and L. H. Kuo, *J. Magn. Magn. Mater.* **165**, 149 (1997).
- ⁹T. Kobayashi, H. Tsuji, S. Tsunashima, and S. Uchiyama, *Jpn. J. Appl. Phys.* **20**, 2089 (1981).
- ¹⁰H. Tsujimoto and Y. Sakurai, *Jpn. J. Appl. Phys.* **22**, 1845 (1983).
- ¹¹N. Smith and W. C. Cain, *J. Appl. Phys.* **69**, 2471 (1991).
- ¹²A. Aharoni, *J. Appl. Phys.* **76**, 6977 (1994).
- ¹³E. E. Fullerton, J. S. Jiang, M. Grimsditch, C. H. Sowers, and S. D. Bader, *Phys. Rev. B* **58**, 12 193 (1998).
- ¹⁴E. E. Fullerton, J. S. Jiang, and S. D. Bader, *J. Magn. Magn. Mater.* **200**, 392 (1999).
- ¹⁵E. Goto, N. Hayashi, T. Miyashita, and K. Nakagawa, *J. Appl. Phys.* **36**, 2951 (1965).
- ¹⁶G. J. Bowden, J. M. L. Beaujour, S. Gordeev, P. A. J. de Groot, B. D. Rainford, and M. Sawicki, *J. Phys.: Condens. Matter* **12**, 9335 (2000).
- ¹⁷For review see: K. H. J. Buschow, *Rep. Prog. Phys.* **40**, 1179 (1977).
- ¹⁸J. J. M. Franse and R. J. Radwanski, in *Handbook of Magnetic Materials*, Vol. 7, edited by K. H. J. Buschow (North-Holland, Amsterdam, 1993), p. 307.
- ¹⁹G. J. Bowden, D. St. P. Bunbury, A. P. Guimaraes, and R. E. Snyder, *J. Phys. C* **1**, 1376 (1968).
- ²⁰V. Oderno, C. Dufour, K. Dumesnil, Ph. Bauer, Ph. Mangin, and G. Marcal, *Phys. Rev. B* **54**, R17 375 (1996).
- ²¹E. Grier, D. Phil. thesis, Oxford University, UK, 2000.
- ²²A. Mougin, C. Dufour, K. Dumesnil, and Ph. Mangin, *Phys. Rev. B* **62**, 9517 (2000).